We emphasize that we have not attempted to construct a detailed mechanism of elementary steps, but have considered only component stoichiometric processes and empirical rate laws as building blocks of the reaction system. Much more information will need to be available on the kinetics of the subsystems before a detailed mechanism of elementary steps for the entire system can be developed.

The present system would seem to be closely related to the iodate–ferrocyanide–sulfite[5] (mixed Landolt, EOE) and bromate–ferrocyanide–sulfite[9] oscillators by the replacement of the halate ion with hydrogen peroxide as oxidant. Although those systems have not yet been analyzed in terms of an alternator model, the fact that both show pH oscillations of 3–5 units in amplitude is suggestive that their dynamics must resemble those of the reaction studied here. If so, the mechanistic insights[5,9,27-29] that have been gained in those systems should be of considerable use in elucidating the mechanism of the hydrogen peroxide–ferrocyanide–sulfite reaction.

Acknowledgment. This work was supported by the National Science Foundation (Grant No. CHE-8800169) and by a U. S.-Hungarian Grant from the NSF (INT-8613532) and the Hungarian Academy of Sciences.

Registry No. H_2O_2, 7722-84-1; SO_3^{2-}, 14265-45-3; $Fe(CN)_6^{4-}$, 13408-63-4.

(27) Gáspár, V.; Showalter, K. *J. Am. Chem. Soc.* **1987**, *109*, 4869.
(28) Edblom, E. C.; Györgyi, L.; Orbán, M.; Epstein, I. R. *J. Am. Chem. Soc.* **1987**, *109*, 4876.
(29) Luo, Y.; Epstein, I. R. *J. Phys. Chem.* **1989**, *93*, 1398.

Low-Temperature Investigation of the Ferrimagnetic Chains $MnM'(EDTA)\cdot 6H_2O$ (M' = Co, Ni, and Cu(II)): Thermal and Magnetic Properties

E. Coronado,*,†,§,[1] M. Drillon,*,† P. R. Nugteren,‡ L. J. de Jongh,‡ D. Beltran,§ and R. Georges⊥

Contribution from the Groupe de Chimie des Matériaux Inorganiques, EHICS, 1 rue Blaise Pascal, 67008 Strasbourg, Cedex, France, Kammerlingh Onnes Laboratorium, P.O. Box 9506, 2300 RA Leiden, The Netherlands, U.I.B.C.M., Departamento Quimica Inorganica, Fac. Ciencias Quimicas, 46100 Burjasot-Valencia, Spain, and L.C.S., Université de Bordeaux I, 351 Cours de la Libération, 33405 Talence, Cedex, France. *Received June 20, 1988*

Abstract: We report on the magnetic and thermal properties of the ordered bimetallic chains $MnM'(EDTA)\cdot 6H_2O$ (M' = Co, Ni, and Cu(II)) in the very low-temperature range. Their structure consists of infinite zigzag chains, built up from two alternating (M,M') sites; furthermore, the M–M' distances along the chain are slightly alternating. The magnetic behavior exhibits the characteristic features of 1-d ferrimagnets with a minimum of X_mT and a divergence upon cooling down. Interchain interactions lead at very low temperature to a long-range antiferromagnetic ordering as outlined by the sharp maximum of X_mT and the λ-peak in the specific heat data. In the 1-d regime, an analysis of the data from Heisenberg and Ising models is reported. It is emphasized that the degree of J-alternation of these compounds varies in the order [MnNi] < [MnCu] ≪ [MnCo]. A qualitative explanation of this trend is given on basis of the structural features and the electronic ground state of the interacting ions. Finally, the 1-d character of these systems is discussed.

One of the most remarkable advances in low-dimensional magnetism has concerned the recent discovery of a new kind of magnetic systems, namely ferrimagnetic chains or 1-d ferrimagnets.[2] These systems are generally defined as 1-d antiferromagnets made up of two different and alternating spin sublattices, thus giving a net magnetic moment in the ground state. They show a distinctive magnetic behavior (1-d ferrimagnetism) characterized by a minimum at an intermediate temperature, which depends on the strength and anisotropy of the magnetic sublattices, and a divergence at lower temperature. Ordered bimetallic chain compounds provide typical examples of this kind, but actually several homometallic systems also show 1-d ferrimagnetism. That has been emphasized in the case of regular spin chains formed by alternating *g*-factors on consecutive sites[3,4] and more recently in some exotic networks of interacting ions.[5,6]

In the last few years, several examples of ordered bimetallic chains have been reported.[7-12] We have participated in this effort both in the design of new 1-d ferrimagnets[13,14] and in the development of models required to understand their properties.[3,4,15-20] The bimetallic compounds isolated belong to the isostructural family $MM'(EDTA)\cdot 6H_2O$ (abbreviated as [MM'], where M = Mn, Co, Ni, and Mg and M' = Co, Ni, Cu, and Zn(II). The

† Groupe de Chimie des Matériaux Inorganiques.
‡ Kammerlingh Onnes Laboratorium.
§ Departamento Quimica Inorganica.
⊥ Université de Bordeaux.

(1) Permanent address: Departamento de Quimica Inorganica Valencia, Spain.
(2) Landee, C. P. In *Inorganic Low Dimensional Crystalline Materials*; Delhaes, P., Drillon, M., Eds.; NATO ASI Series; Plenum: New York, Vol. B 168, p 75.
(3) Coronado, E.; Drillon, M.; Fuertes, A.; Beltran, D.; Mosset, A.; Galy, J. *J. Am. Chem. Soc.* **1986**, *108*, 900.
(4) Coronado, E.; Drillon, M.; Beltran, D.; Bernier, J. C. *Inorg. Chem.* **1984**, *23*, 4000.
(5) Landee, C. P.; Djili, A.; Place, H.; Scott, B.; Willett, R. D. *Inorg. Chem.* **1988**, *27*, 620.
(6) Drillon, M.; Coronado, E.; Belaiche, M.; Carlin, R. *J. Appl. Phys.* **1988**, *63*, 3551.
(7) Gleizes, A.; Verdaguer, M. *J. Am. Chem. Soc.* **1981**, *103*, 7373; **1984**, *106*, 3727.
(8) Verdaguer, M.; Julve, M.; Michalowicz, A.; Kahn, O. *Inorg. Chem.* **1983**, *22*, 2624.
(9) Pei, Y.; Sletten, J.; Kahn, O. *J. Am. Chem. Soc.* **1986**, *108*, 9143.
(10) Pei, Y.; Verdaguer, M.; Kahn, O.; Sletten, J.; Renard, J. P. *Inorg. Chem.* **1987**, *26*, 138.
(11) Pei, Y.; Verdaguer, M.; Kahn, O.; Sletten, J.; Renard, J. P. *J. Am. Chem. Soc.* **1986**, *108*, 7428.
(12) Pei, Y.; Kahn, O.; Sletten, J.; Renard, J. P.; Georges, R.; Gianduzzo, J. C.; Curely, J.; Xu, Q. *Inorg. Chem.* **1988**, *27*, 47.
(13) Beltran, D.; Escriva, E.; Drillon, M. *J. Chem. Soc., Faraday Trans. II* **1982**, *78*, 1773.

0002-7863/89/1511-3874$01.50/0

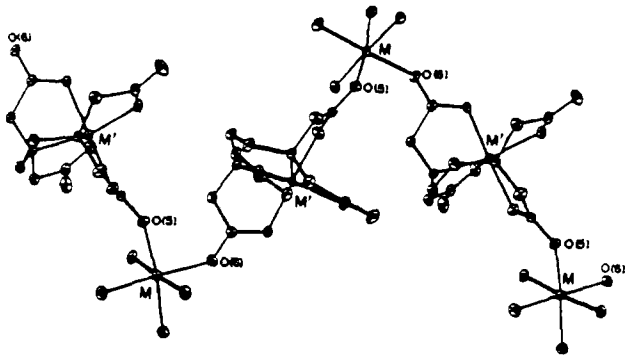

Figure 1. View of the alternating bimetallic chain in the MM'-(EDTA)·$6H_2O$ complexes.

structure of these compounds (Figure 1) consists of infinite zigzag chains built up from two alternating octahedral sites denoted as "hydrated" or "chelated" according to local environments.[3] In the former, M is coordinated to four water molecules and the oxygen atoms of carboxylate groups, while in the latter M' is hexacoordinated by the EDTA ligand. In bimetallic compounds both sites are selectively occupied by metal ions giving rise to bimetallic ordered chains. On the other hand, slight alternating M–M' distances occur along the chain which are related to different bridging carboxylate topologies.

The alternating chain may then be schematically illustrated as

$$--M(H_2O)_4O_2—M'(EDTA)--M(H_2O)_4O_2—M'(EDTA)$$

where dashed and full lines refer to alternating metallic distances.

It is worth noticing that many choices of metals can easily be accommodated without significant structural change. So, this family constitutes an ideal structural support for investigating a wide variety of 1-d ferrimagnets, with Ising or Heisenberg exchange coupling. Moreover, the alternating metal distances along the chain can give rise to an alternation in the exchange parameter.[21,22]

In this paper, we present the magnetic susceptibility and specific heat measurements of the [MnM'] series (M' = Cu, Ni, and Co(II)), characterized by two very different alternating spins. In the very low-temperature range, these properties are shown to be strongly dependent on the interchain interactions, which are particularly enhanced in the present case because of the high-spin ground state of each ferrimagnetic chain. These interactions lead to a phase transition toward an antiferromagnetic 3-d ordering with sharp maxima of X_mT and C_p at a critical temperature, T_c. We report in this paper an analysis of the data in the 1-d regime on the basis of ferrimagnetic Heisenberg and Ising models including in the last case an alternation in the exchange parameter. We also discuss the 1-d character of these systems.

Experimental Section

EPR measurements were recorded on a Bruker ER 200D X-band spectrometer.

Susceptibility measurements were performed in the temperature range 0.15–4.2 K using two different techniques. The low-temperature data wre recorded in an adiabatic demagnetization apparatus by means of a mutual inductance bridge operating at 35 Hz. The susceptibility data, obtained in arbitrary units, were first corrected for the signal of the empty coil system and then scaled in the range 0.15–2.1 K onto the results obtained in a differential susceptibility set-up operating at 82.8 Hz in the temperature range 1.3–4.2 K. The data, corrected for the diamagnetism of the constituent atoms, are given with an accuracy better than 10^{-5} emu·mol^{-1} for the susceptibilities and a temperature uncertainty of 0.01 K.

Specific heat measurements were performed in the temperature range 0.07–30 K. Conventional heat-pulse techniques have been used. The low-temperature specific heat data (0.07–1.5 K) were taken in an adiabatic demagnetization apparatus using magnetic thermometry. The

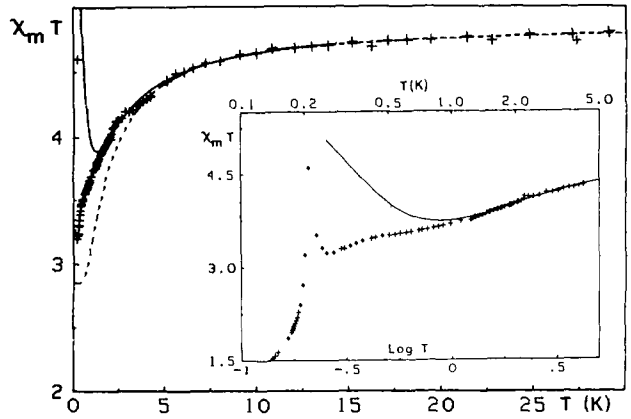

Figure 2. Magnetic behavior of [MnCu]. The theoretical variation of a [$^5/_2$ – $^1/_2$] Heisenberg closed chain (N = 3) is reported as a solid line in the figure (J/k = –0.5 K). The behavior of an isolated dimer is given in dashed line (J/k = –0.45 K).

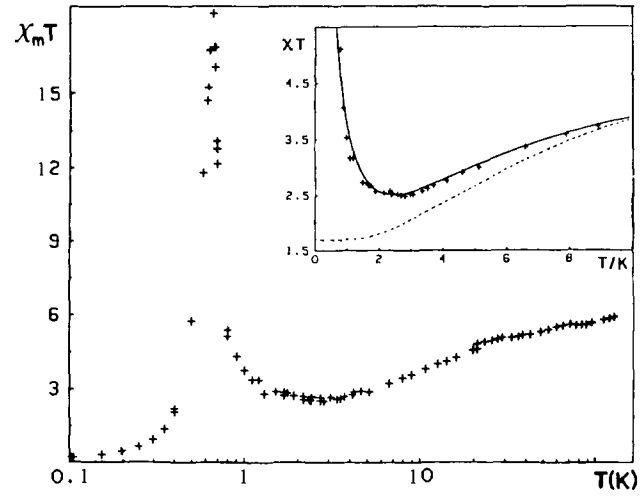

Figure 3. Magnetic behavior of [MnNi]. Full and dashed lines correspond to the fits from [$^5/_2$ – 1] Heisenberg chain and dimer limits, respectively.

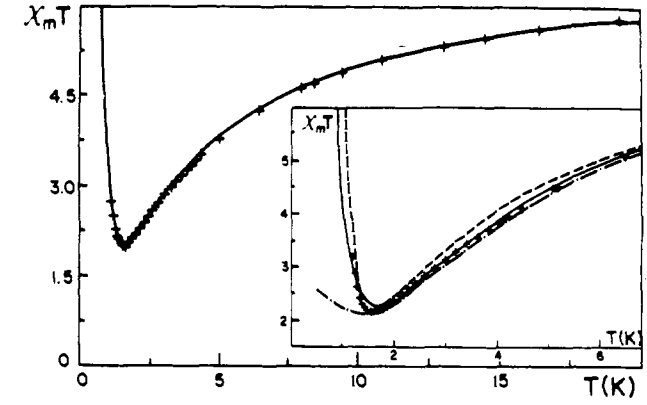

Figure 4. Magnetic behavior of [MnCo]. Solid line corresponds to the best fit from the J alternating [$^5/_2$ – $^1/_2$] Ising chain model. Comparison to uniform chain (– –) and dimer (–·–) limits is given in the inset.

(14) Escriva, E.; Fuertes, A.; Beltran, D. *Transition Met. Chem.* **1984**, *9*, 184.
(15) Drillon, M.; Coronado, E.; Beltran, D.; Curely, J.; Georges, R.; Nugteren, P. R.; de Jongh, L. J.; Genicon, J. L. *J. Magn. Magn. Mater.* **1986**, 54–57, 1507.
(16) Drillon, M.; Coronado, E.; Beltran, D.; Georges, R. *J. Appl. Phys.* **1985**, *57*, 3353.
(17) Drillon, M.; Coronado, E.; Beltran, D.; Georges, R. *Chem. Phys.* **1983**, *79*, 449.
(18) Drillon, M.; Gianduzzo, J. C.; Georges, R. *Phys. Lett.* **1983**, *96A*, 413.
(19) Georges, R.; Curley, J.; Drillon, M. *J. Appl. Phys.* **1985**, *58*, 914.
(20) Curely, J.; Georges, R.; Drillon, M. *Phys. Rev. B* **1986**, *33*, 6243.
(21) Coronado, E.; Nugteren, P. R.; Drillon, M.; Beltran, D.; de Jongh, L. J.; Georges, R. In *Organic and Inorganic Low Dimensional Crystalline Materials*; Delhaes, P., Drillon, M., Eds.; NATO ASI Series, Plenum: New York, 1987; Vol. B 168, p 405.

Table I. Magnetic and Thermal Features of the [MnM'] Series

compd	T_{min} (K)	$[X_mT]_{min}$	T_{max} (K)	T_c (λ-peak) (K)
[MnCu]	0.28	0.32	0.21	0.20
[MnNi]	2.7	2.5	0.66	0.65
[MnCo][a]	1.6	1.98		1.06

[a] In this system the peak of X_m has not been observed since the measurements have been performed down to 1.3 K.

powdered samples were mixed with Apiezon-N grease for thermal contact. A pumped ^{4}He apparatus equipped with a mechanical heat switch was used for the high-temperature measurements (1.4–30 K), using germanium thermometry. A small amount of ^{3}He gas was used to ensure thermal contact between the sample and the calorimeter.

Results

The powder susceptibility data of the title compounds are reported through a plot of $X_mT = f(T)$ in Figures 2–4; X_m is the magnetic susceptibility per mol. The three compounds show a typical 1-d short range ferrimagnetic behavior (minimum and divergence of X_mT). At a critical temperature (T_c), a sharp peak of X_mT is observed in [MnCu] and [MnNi] systems suggesting a transition to long-range magnetic ordering. Such an assumption is unambiguously confirmed by the heat capacity data which show λ-type anomalies at the same temperatures (Figure 5). In turn, the slight bump outlined in the C_p data is to be attributed, according to magnetic findings, to the 1-d magnetic contribution. On the other hand, an additional contribution arising from nuclear hyperfine interactions appears at very low temperatures (below 0.3–0.4 K), giving rise to a T^{-2} tail. Finally, the increase of the specific heat above 6 K corresponds to the lattice contribution (solid line on Figure 5). The characteristic features of these systems are summarized in Table I.

In discussing the properties of these compounds we have to consider first the electronic ground states of the interacting ions which determine, to a large extent, the symmetry of the exchange Hamiltonian. Spin free octahedral manganese(II) is characterized by a $^6A_{1g}$ ground term giving an isotropic g value of 2.0, as observed by EPR in [MnZn]. Conversely, the ground state $^3A_{2g}$ of nickel(II) is split in distorted octahedral environments. Specific heat measurements carried out on a Ni-doped [MgZn] sample allow us to estimate the separation between the spin singlet I0> and the doublet I ± 1> as $\Delta E = 8.7$ K. This value is large enough to prevent the observation of the EPR absorption at X-band. Anyway, g values of this ion in similar environments are commonly found to be isotropic or nearly so and typically close to 2.25–2.30.[23] Lastly, the electronic properties of copper(II) and cobalt(II) occupying the "chelated" site have been previously discussed.[22] A quasi isotropic g value (with $g_\parallel = 2.27$ and $g_\perp = 2.02$) is observed for the copper(II) spin doublet, while a very large anisotropy ($g_1 = 10.1$, $g_2 = 1.43$, $g_3 = 1.24$) results for the cobalt(II) doublet.

Analysis of the [MnCu] and [MnNi] Heisenberg Ferrimagnetic Chains

Magnetic Properties. Owing to the ground state of the interacting ions, these systems are assumed to be well-described by the fully isotropic Heisenberg Hamiltonian

$$\mathcal{H}_{ex} = -J\sum S_{2i}(S_{2i-1}+S_{2i+1})$$

where the spin operator S_k takes values $S_a = {}^5/_2$ and $S_b = {}^1/_2$ for even and odd sites, respectively. Further, in studying magnetic susceptibility, alternating Landé factors are to be introduced in the Zeeman term

$$\mathcal{H}_z = -(g_a\sum S^z_{2i-1} + g_b\sum S^z_{2i})\mu_B H_z$$

The solutions of this Hamiltonian were shown to be available in the classical limit, $S = \infty$, only.[17] The calculated expression is given in Chart I.

For quantum spin systems numerical solutions of X_m can be obtained by extrapolating the results performed on 2N site rings

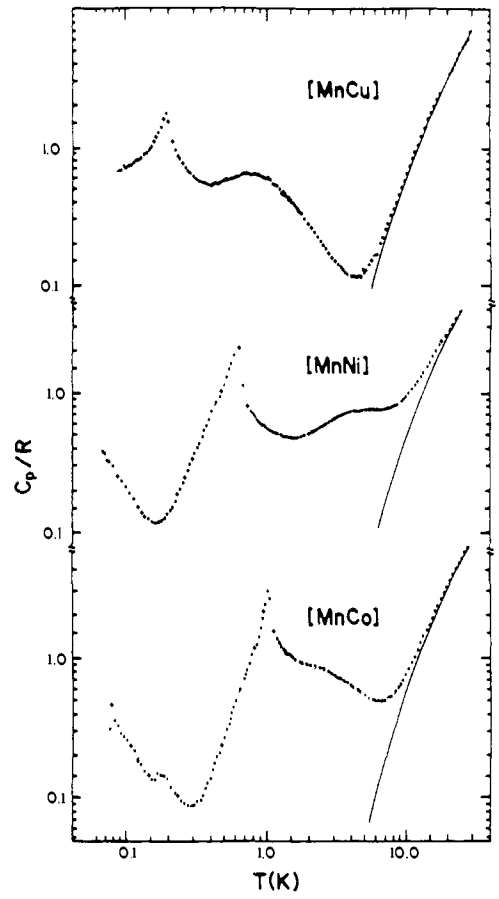

Figure 5. Specific heat data of the [MnM'] compounds. Full line corresponds to the specific heat of the isomorphous nonmagnetic compound [ZnZn].

of increasing size to the thermodynamic limit ($N \rightarrow \infty$). In this respect, we have developed a general computing program that takes fully into account the geometrical and spin space symmetries of the rings in order to reduce the computational work.[18]

Clearly, in such a kind of treatment, the computations are limited by the size of the matrices to be diagonalized and the required computing times. So, the large spin multiplicities involved in the systems of interest (abbreviated as [$^5/_2$ – $^1/_2$] and [$^5/_2$ – 1]) allowed us to perform the calculations up to $N = 3$ pairs only.[24] This fact makes the extrapolation procedure more difficult here than in systems with smaller spin multiplicities (for example, in systems [S – $^1/_2$] with $S < {}^5/_2$), the computation of which can be performed at least up to $N = 4$.[16]

In the present case any extrapolation result may be questionable since we only used two values of N, while the procedure needs at least a sequence of three values (extrapolation on similar systems show that the value corresponding to $N = 1$ is to be ruled out[25]). Anyway, we observe that the data for large S converge more rapidly as a function of N than those for small S. Thus, in both systems the convergence is rather rapid above the temperature of the X_mT minimum (Figure 6), suggesting that above this temperature the curve for $N = 3$ describes the limiting behavior with a good accuracy. Hence, in a large temperature region, the numerical results obtained for the $N = 3$ rings can be used to fit the experimental data. In Figure 6, X_n represents the normalized susceptibility per spin pair defined as $[10X_m]/[(N\mu_B/k)(g_aS(S + 1) + g_bS'(S' + 1))]$. An estimate of the exchange coupling can be deduced for both [$^5/_2$ – $^1/_2$] and [$^5/_2$ – 1] chains from the coordinates of the X_mT minimum (listed in Table II).

On the other hand, it is clear that the classical spin model should conveniently describe the behavior of ferrimagnetic chains made

(22) Coronado, E.; Drillon, M.; Nugteren, P. R.; de Jongh, L. J.; Beltran, D. *J. Am. Chem. Soc.* **1988**, *110*, 3907.
(23) McGarvey, B. R. *Transition Met. Chem.* **1966**, *3*, 89.
(24) Calculations were performed on a UNIVAC 1110 machine.
(25) Coronado, E.; Drillon, M.; Georges, R., to be published.

Chart I. Analytical Expressions of the Magnetic Susceptibility and Specific Heat for the Classical Heisenberg Chain (Expression 1) and the Alternating [$S - {}^1/_2$] Ising Chain (Expressions 2 and 3)[a]

expression 1

$$X_m = \frac{N\mu_B^2}{3kT}\left[g_+^2 \frac{1 + F(\beta J)}{1 - F(\beta J)} + g_-^2 \frac{1 - F(\beta J)}{1 + F(\beta J)} \right]$$

with $g_\pm = {}^1/_2(g_a \pm g_b)$; $F(\beta J) = \coth(\beta J) - 1/\beta J$; $\beta = 1/kT$

expression 2

$$C_p/R = \beta^2[Z''/Z - Z'^2/Z^2]$$

expression 3

$$X_\parallel = N/\beta\left[S_0'' + \frac{S_0 S_0'' - 2P_0''}{(S_0^2 - 4P_0)^{1/2}} \right] \Big/ [S_0 + (S_0 - 4P_0)^{1/2}]$$

with $$Z = \sum_j^S (2 - \delta j_0)[\cos h(\beta j J_+] + \cos h[\beta j J_-]; \quad J_\pm = {}^1/_2(J \pm J')$$

$$Z' = \sum_j^S j(2 - \delta j_0)[J_+ \sin h[\beta j J_+] + J_- \sin h[\beta j J_-]]$$

$$Z'' = \sum_j^S j^2(2 - \delta j_0)[J_+^2 \cos h[\beta j J_+] + J_-^2 \cos h[\beta j J_-]]$$

$$S_0 = 2\sum_j^S (2 - \delta j_0)\cos h(\beta j J_+)$$

$$S_0'' = 2\sum_j^S (2 - \delta j_0)[[g_a\mu_B\beta/2]^2 + j^2[g_b\mu_B\beta]^2]\cos h(\beta j J_+) + j g_a g_b \mu_B^2 \beta^2 \sin h[\beta j J_+]$$

$$P_0 = \sum_{j,k}^S (2 - \delta j_0)(2 - \delta k_0) \times [\cos h(\beta j J_+)\cos h(\beta k J_+) - \cos h(\beta j J_-)\cos h(\beta k J_-)]$$

$$P_0'' = (g_b\mu_B\beta)^2 \sum_{j,k}^S (2 - \delta j_0)(2 - \delta k_0)[(j^2 + k^2) \times [\cos h(\beta j J_+)\cos h(\beta k J_+) - \cos h(\beta j J_-)\cos h(\beta k J_-)] - 2jk[\sin h(\beta j J_+)\sin h(\beta k J_+) - \sin h(\beta j J_-)\sin h(\beta k J_-)]]$$

[a] Where the summations extend over j, $k = 0({}^1/_2)$ to S. j_0 and k_0 correspond to kronecker symbols.

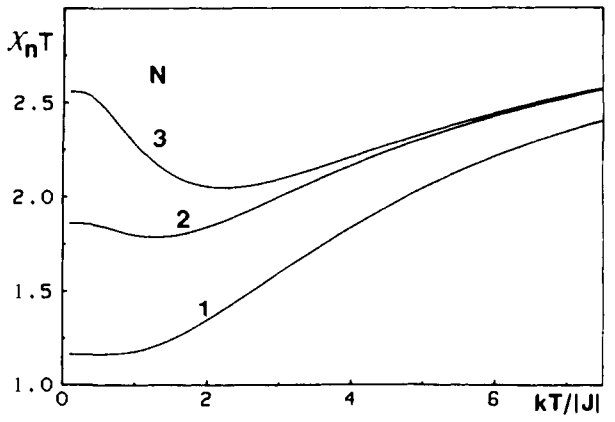

Figure 6. [$^5/_2 - 1$] Heisenberg chain. Magnetic behavior of finite closed chains (length 2N) computed for $g_a/g_b = 1$. X_n is the normalized susceptibility (defined in the text).

Table II. Magnetic and Thermal Features of (S–S') Ferrimagnetic Chains (S = $^5/_2$; S' = $^1/_2$ of 1; $g_a = g_b$)

	Heisenberg model		Ising model
	($^5/_2 - {}^1/_2$)	($^5/_2 - 1$)	($^5/_2 - {}^1/_2$)
$[X_mT]_{min}/(Ng^2\mu_B^2/k)$	2.65	2.3	2.82
$kT_{min}/\|J\|$	2.9	2.3	4.14
C_{pmax}/R	0.7	1.4	0.68
$kT_{max}/\|J\|$	1.4	1.8	1.723

up of large spins. A comparison between the results of quantum (with $N = 3$) and classical treatments is displayed in Figure 7

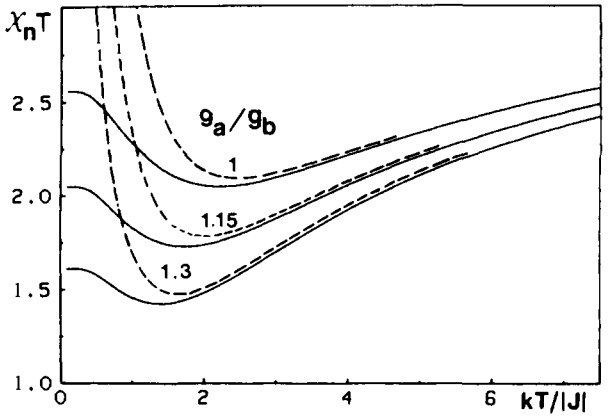

Figure 7. Comparison between quantum ($N = 3$; solid line) and classical (dashed line) [$^5/_2$ -1] Heisenberg chains showing the influence of a g alternation.

Table III. Best Fit Parameters of [MnM'] from Magnetic Susceptibility and Specific Heat Data[a]

		$X_m = f(T)$			$C_p/R = f(T)$
		$-J/k$ (K)	g_{Mn}	$g_{M'}/g_{Mn}$	$-J/k$ (K)
[MnCu]	dimer	0.45	1.95	1.15	0.35
	uniform chain[b]	0.5 (0.35)	1.96 (2.0)	1.15 (1.15)	0.45
[MnNi]	dimer	1.5	2.0	1.23	1.70
	uniform chain	1.5 (1.85)	1.95 (2.0)	1.23 (1.24)	2.25
[MnCo]	dimer	3.4	2.0	2.50	<5
	uniform chain	1.6	1.74	3.39	<3
	altern chain[c]	2.7 (0.6)	1.86	2.96	

[a] In the Hamiltonian the exchange constant is written as $-J$. [b] Inside the parentheses are the values resulting from the high temperature fit (see text). [c] The value inside the parentheses corresponds to J'.

for the [$^5/_2 - 1$] system. We note that both the height and the position of the minimum are in close coincidence whatever the ratio between Landé factors. Hence, this approach can be convenient to fit the data of [MnNi] in all of the 1-d regime.

The analysis of the [MnCu] data has been made for $g_{Cu}/g_{Mn} = 1.15$, in agreement with EPR results. In Figure 2 and Table III are reported the results of two different fits; one takes into account the data over the whole temperature range (dashed line), and the other only data below 5 K (solid line of the inset). The former fit gives an exchange parameter $J = -0.5$ K (g_{Mn} was set equal to 2); in the later the resulting parameters are $J = -0.35$ K and $g_{Mn} = 1.96$. We observe that at temperature around the minimum, both fits disagree significantly with the experiment; thus, while theory predicts a divergence of the product X_mT below 1 K, the experimental data decrease continuously with T down to 0.3 K (see inset on Figure 2)). The origin of this discrepancy may lie within the structure of this type of chains. Recall that the M–M' distances along the chain are slightly alternating in all the members of the EDTA family. For example, in [MnCu] the two consecutive Mn–Cu distances are 5.461 and 6.122 Å. This feature should entail an alternation in the exchange parameters, which has been ignored in the above analysis. The extent of dimerization of the chain can be estimated by comparing the behavior of a uniform bimetallic chain ($J = J'$) and a bimetallic dimer ($J = -0.45$ K, $J' = 0$). We observe that while the chain behavior well reproduces the experiment down to 1 K, the dimeric behavior is much below the experimental data, even at 4 K. This suggests that the J alternation remains weak.

The analysis of the [MnNi] data has been made from the classical spin model, by introducing in expression 1 of Chart I the following scaling factors.

$$J \rightarrow J([S(S+1)S'(S'+1)]^{1/2}$$

$$g_i \rightarrow g_i[S_i(S_i+1)]^{1/2}, \qquad \text{with i = a or b}$$

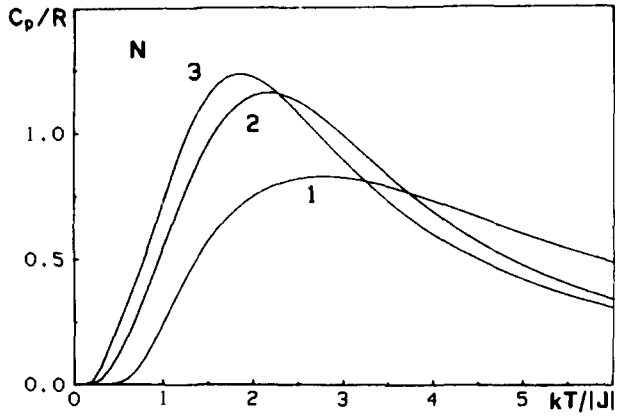

Figure 8. [$^5/_2$ - 1] Heisenberg chain. Specific heat per spin pair of finite closed chains of length $2N$.

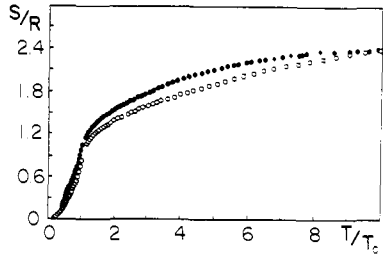

Figure 9. Magnetic entropy of the [MnCu] (●) and [MnNi] (○) compounds.

A very satisfying description of the experiment, in the region of the X_mT minimum (i.e., below 10 K), is obtained with the following set of parameters: $J/k = -1.5$ K, $g_{Mn} = 1.95$, and $g_{Ni} = 2.39$ (solid line of the inset of Figure 3). This fit reproduces both the position and the height of the susceptibility minimum (2.7 K and 2.5 emu·mol^{-1}·K, respectively); however, its quality is not preserved at higher temperatures and further, the resulting value of g_{Mn} is slightly low. The fit over the whole temperature range (above 2.3 K), by keeping constant $g_{Mn} = 2$, gives a slightly larger exchange parameter ($J/k = -1.85$ K). Conversely, the quality of this fit is less satisfactory in the region of the minimum which is expected at 3.2 K and 2.8 emu·mol^{-1}·K. These results are listed in Table III. The presence of a slight J alternation or other factors like zero-field splitting of Ni(II) ion or the quantum nature of the spins could be the origin of this discrepancy.

Thermal Properties. In discussing the specific heat data, it is to be noted that the theoretical curves for finite closed chains show a more complicated convergence than those of the magnetic susceptibility. They display crossings at low temperature (Figure 8) which prevent any extrapolation in this region. Hence, only a rough estimate of the position of the maximum can be made by assuming that in both systems the evolution in this with N is similar to that found in [$S - {}^1/_2$] and [$S - 1$] systems, with $S < {}^5/_2$) (Table II).

Specific heat data of [MnCu] and [MnNi] are displayed in Figures 10 and 11. They correspond to the magnetic contributions obtained after subtracting from the experimental data the lattice contribution (estimated making use of the specific heat of the isomorphous diamagnetic compound $Zn_2(EDTA)\cdot 6H_2O$) and the hyperfine contribution. Due to the occurrence of 3-d ordering transition, a significant part of the magnetic entropy must be involved in long-range order (i.e., below T_c). Accordingly, we have plotted in Figure 9 the magnetic entropy of these systems as a function of temperature. Note that, although in both systems the entropy content of the magnetic contribution is in good agreement with the expected value, $S/R = \ln(2S + 1) + \ln(2S' + 1)$, around 40% of S/R is already displayed at T_c. Consequently, the height of the 1-d Schottky anomalies is expected to be significantly lower than expected. In regard to the temperature of the maxima, it is reasonable to assume that its stays nearly unaffected, since the peaks overlap weakly with Schottky anomalies. Then, in the analysis of the data, only the position of the maxima will be considered as relevant. In this respect, we have compared in Figures 10 and 11 the experimental data to the theoretical behaviors of a bimetallic dimer (solid line) and a $N = 3$ closed chain (dotted line). In order to make easier the comparison, the theoretical curves have been corrected by a scaling factor (0.85 in [MnCu] and 0.91 in [MnNi]) in such a way that the curve of the dimer matches the experimental Schottky anomaly. Bearing in mind the limitations imposed by theory and experiment, it is evident that these results do not allow one to extract any information about the degree of dimerization of these chains. Nevertheless, it is worth noticing that the exchange parameters agree reasonably well with those calculated from magnetic data. (Table IV).

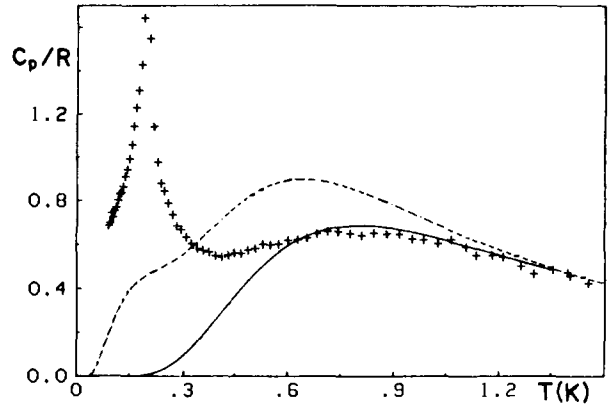

Figure 10. Magnetic specific heat of [MnCu]. Dashed and full lines correspond to the theoretical behaviors of a [$^5/_2$ - $^1/_2$] Heisenberg closed chain ($J/k = -0.45$ K) and dimer ($J/k = -0.35$ K), respectively.

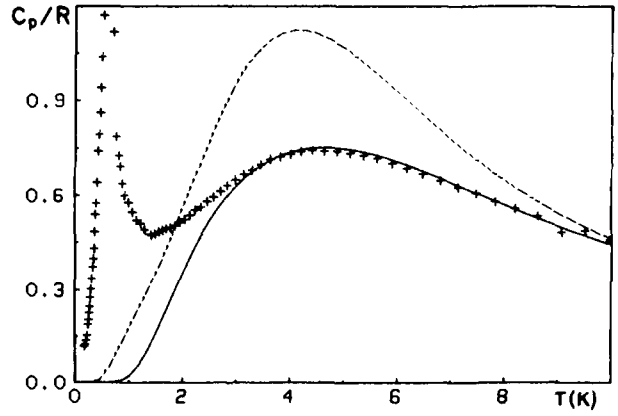

Figure 11. Magnetic specific heat of [MnNi]. Dashed and full lines corresponds to the theoretical behaviors of a [$^5/_2$ = 1] Heisenberg closed chain ($J/k = -2.25$ K) and dimer ($J/k = -1.70$ K), respectively.

Analysis of the [MnCo] Ising Ferrimagnetic Chains

Magnetic Properties. Due to the combined effect of spin-orbit coupling and local distortion of the octahedral sites, it is appropriate to describe high-spin cobalt(II), at low enough temperatures (<20–30 K), by an anisotropic Kramers doublet with effective spin $S = {}^1/_2$. This large anisotropy (reflected in the g tensor) entails an effective anisotropy of the exchange coupling.[26] Then, an anisotropic exchange model is expected to be convenient in describing the magnetic and thermal properties.

We will focus in the following on the fully anisotropic Ising model whose exact solutions can be derived. Assuming two alternating exchange couplings between nearest neighbors, J and J', we have developed[27] a general treatment for the two spin

(26) See de Jongh, L. J. In *Magneto-Structural Correlations in Exchange-Coupled Systems*; Gatteschi, D.; Kahn, O.; Willett, R. D.; Eds.; NATO Advanced Studies Institute, Reidel: Dordrecht, 1984.

(27) Sapina, F.; Coronado, E.; Georges, R.; Beltran, D.; Drillon, M. *J. Phys.*, in press.

Table IV. Magnetic Characterization of the MM'(EDTA)·6H₂O Family[a]

compd	Spins ($S - S'$)	Exchange J/k (K)	comments	intermetallic distances[b]	ref
[MnCu]	$^5/_2 - ^1/_2$	−0.5 (H)	weak J alternation	5.581–6.122	this work
[MnNi]	$^5/_2 - 1$	−1.5 (H)	J uniform chains		this work
[MnCo]	$^5/_2 - ^1/_2$	−0.6 (I)	J alternating chains ($J'/J = 0.22$)	5.392–6.061	this work
[NiNi]	1 − 1	−8.3 (H)	J uniform chains	5.517–5.890	3
[CoCo]	$^1/_2 - ^1/_2$	−6.3 (A)	"quasi" isolated dimers ($J'/J < 0.01$)	5.581–5.994	22
[CoCu]	$^1/_2 - ^1/_2$	−2.7 (A)	"quasi" isolated dimers ($J'/J < 0.02$)		22

[a] The letters inside the parentheses refer to the symmetry of the interaction Hamiltonian: (H), Heisenberg; (I), Ising; (A) anisotropic exchange. Scaling factors have been considered in J to account for the effective spin doublet of Co(II) [b] From ref 3.

sublattice chain [$S - ^1/_2$] by using the transfer matrix technique.[22] Closed formulas of the thermodynamic quantities of interest (parallel component of the zero-field susceptibility and specific heat) have been derived (Chart I).

In the case under consideration, the expression for the perpendicular susceptibility cannot be determined by the same procedure. However, the fact that the perpendicular contribution is weak, (proportional to $g_\perp^2$), varies in a limited range at low enough temperature, and decreases toward zero upon cooling down, implies that $X_\perp$ contributes to the average susceptibility as a small additional contribution. Hence, the ferrimagnetic behavior must come as a whole from the parallel component of the susceptibility; so, it is reasonable to assume that the experimental data are, to a large extent, accounted for by this component.

The low-temperature data are illustrated in Figure 4, along with the best-fitted curves. A very close agreement with experiment has been obtained with the following set of parameters: J/k = −2.7 K, J'/k = 0.6 K, g_{Co} = 5.5, and g_{Mn} = 1.86, which indicates a significant J alternation along the chain. In order to examine the validity of the above result, we have fit the data to a bimetallic dimer ($J' = 0$) and a uniform bimetallic chain ($J = J'$) model. The resulting parameters are listed in Table III. We observe that the dimeric behavior well reproduces the decrease of X_mT upon cooling down and the position of the minimum but does not allow one to explain the sharp divergence at lower temperature. Conversely, the uniform chain behavior gives a close agreement with the experiment for temperatures around and below the minimum but is less satisfactory at intermediate temperature (in the range 2–8 K) (see inset of Figure 4).

Thermal Properties. The magnetic contribution of the specific heat of [MnCo] is displayed in Figure 12. In the present case the λ-peak is closer to the Schottky anomaly than in the case of [MnCu] and [MnNi] (see Figure 5). This prevents the analysis of the data from the theoretical expression obtained for a J alternating Ising chain (Chart I). Anyway, these measurements may be useful to estimate the limiting values of J. Thus, assuming that the maximum of the Schottky anomaly is at about 2 K, a J value around −3 and −5 K may be predicted from the dimer and the chain models. In Figure 12 are plotted the theoretical curves for dimer (solid line) and chain (dashed line) limits showing J values determined from magnetic data. We observe that a maximum of C_p/R around 1.5 is predicted, in close coincidence with the experimental results.

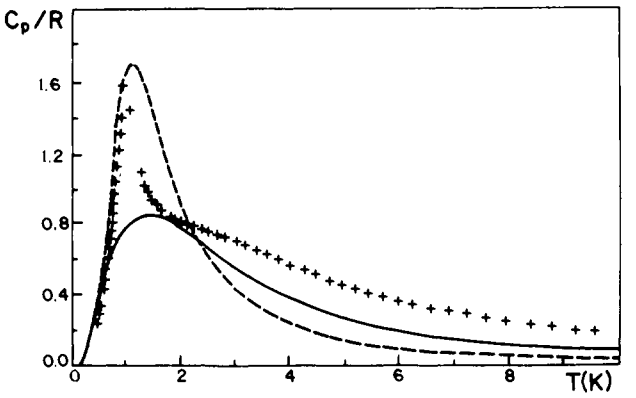

Figure 12. Magnetic specific heat of [MnCo]. Dashed and full lines correspond to the theoretical behaviors of a [$^5/_2 - ^1/_2$] Ising chain and dimer. The J values are those obtained from magnetic data.

Discussion

In this paper, we have reported the low-temperature results of magnetic and thermal properties of the isostructural bimetalic series MnM'(EDTA)·6H₂O (M' = Cu, Ni, and Co(II)). In accordance with their structure, these compounds exhibit the characteristic magnetic behavior of 1-d ferrimagnets with a minimum of X_mT and a divergence upon cooling down. Their one-dimensional character is limited by the interchain interactions which lead to a 3-d antiferromagnetic ordering at a critical temperature, T_c, clearly noticeable by both susceptibility and specific heat measurements. These features are summarized in Table I.

In the one-dimensional regime, the experimental results have been discussed according to the electronic ground state of the interacting ions, in terms of isotropic (Heisenberg) or anisotropic (Ising) models. Thus, [MnCu] and [MnNi] have been modeled assuming an isotropic exchange along a chain of alternating spins ([$^5/_2 - ^1/_2$] and [$^5/_2 - 1$], respectively) and Landé factors. Under such an assumption, only asymptotic solutions of the magnetic susceptibility and specific heat have been obtained through a numerical procedure, similar to that reported for the $S = ^1/_2$ antiferromagnetic chain.[28] Due to the large spin multiplicites involved in these systems, this procedure leads to a poor accuracy of the results for the very low-temperature behavior. An alternative formalism based on classical spins has shown to be well adapted for describing the susceptibility of the [$^5/_2 - 1$] ferrimagnetic chain (Chart I); accordingly, it has been successfully employed to analyze the magnetic data of [MnNi].

The case of [MnCo] has been modeled assuming fully anisotropic exchange interactions. Such an assumption would seem too drastic since Mn(II) is isotropic, and, hence, only Co(II) promotes an anisotropic exchange. This situation is quite similar to that found in [CoCu], in which the anisotropic ("hydrated") Co(II) ion is alternating with the "quasi" isotropic Cu(II) ion. In that case a large anisotropy was determined ($J_\perp/J_\parallel = 0.35$).[22] Taking into account that in the present case the ("chelated") Co(II) is more anisotropic, a larger exchange anisotropy is to be expected, which justifies the above assumption. Exact solutions of the magnetic susceptibility and specific heat for the J alternating Ising chain [$S - ^1/_2$] have been given and applied successfully to the specific case of $S = ^5/_2$.

Although in the analysis of the [MnM'] systems several factors, like interchain interactions, alternating exchange interactions, or zero-field splitting of Ni(II) have been ignored, a reasonable agreement between the exchange parameters determined from the two experiments has been obtained. On the other hand, this analysis has allowed us to emphasize significant differences in the degree of J alternation (J'/J). Thus, while [MnNi] behaves as a uniform chain ($J'/J = 1$), in [MnCu] the effect of a slight J alternation is clearly noticeable in the low-temperature magnetic behavior; in regards to the [MnCo] system, a significant dimerization of the chain has been determined ($J'/J = 0.22$).

The observed trend can be completed with the results obtained on other members of the EDTA family and are summarized in Table IV. We notice that the degree of alternation varies from

(28) Bonner, J. C.; Fisher, M. E. *Phys. Rev.* **1964**, *135*, A640.

about 0.01 in the "quasi" isolated dimers [CoCo] and [CoCu], to 1 in the uniform chains [MnNi] and [NiNi]. Obviously, this variation is too large to be attributed only to slight inequivalences in the intermetallic distances and angles. In fact, the actual mechanism of the exchange is orbital in nature, so that an electronic reason could be invoked. Thus, one would expect that the isotropic Mn(II) ion will be much less sensible to small structural changes within the chain than the Cu(II) ion. That is due to the fact that while in Mn(II) the five d-orbitals are magnetically active, in Cu(II) only the $d_{x^2-y^2}$ orbital is interacting. An intermediate situation is expected for the Ni(II) ion, which disposes of two e_g orbitals. This argument allows us to explain the larger alternation observed in [MnCu] with respect to [MnNi].

The drastic alternation found in the compounds containing Co(II) is difficult to understand in the above terms; it is likely related to the orbital degenerancy of this ion. So far, the orbital models proposed to describe the interaction in bimetallic systems have assumed an isotropic exchange between nondegenerate metallic ions.[29] For the case of degenerate ions their spin anisotropy (reflected in the g tensor) entails an effective exchange anisotropy; hence, we anticipate that the exchange compounds between two ions will be largely dependent on the relative orientation of their g tensors. In our case, due to the structural features of the zigzag chains the g tensors of each three consecutive sites M–M′–M (see Figure 1) must present different orientations with respect to the principal magnetic axes. When dealing with isotropic ions, this fact is irrelevant and a J alternation can only come from a structural effect. However, if one of the two ions is anisotropic, two different J_z values are expected, even in the absence of structural alternation. This result may be equally understood in terms of an orbital model: thus, if M′ is the Co(II) ion, the anisotropic distribution of the spin density around this ion can give rise to different overlaps with the magnetic orbitals of the two neighboring M ions and consequently to two different exchange interactions. From a general viewpoint, it can be predicted that alternating exchange between consecutive sites –M–M′–M–M′– is related to the lack of symmetry on both sites. This effect should be greatly enhanced as the anisotropy of interacting ions increases.

Finally, as regards the interchain interactions, it is worth noticing that their influence is quite prominent in the [MnM′] series, while they are negligible in the regular spin compounds [CoCo], [CoCu], and [NiNi] (no transition to a long-range magnetic ordering was observed in specific heat measurements). Such a difference is closely related to the ground spin configuration of these chains. Thus, though the interchain interactions between high-spin ground-state chains represent a first-order effect, they act in turn to second order when only g factors alternate (the ground configuration is then $S = 0$).

In view of this striking difference it can be of interest to compare the 1-d character of several of the [MnM′] compounds. Whatever the system, the crystal structure shows that the chains are well isolated with the shortest intermetallic distance between neighboring chains around 6 Å[3]. Then, we can assume that the isolation of the chains is similar, in the three reported compounds, with the interchain interactions (j) remaining much smaller than the intrachain ones (J). An estimate of the 1-d character is provided by the ratio j/J. In the case of a Heisenberg classical chain, Richards[30] has proposed an analytical expression which relates this ratio to the critical temperature T_c, the main exchange parameter J, and the local spin S

$$T_c = (2J/k)S(S + 1)(j/J)^{1/2}$$

Modifying this expression to account for the two different local spins involved, that is by changing $S(S + 1)$ by $[S(S + 1)S'(S' + 1)]^{1/2}$, we obtain $j/J = 0.2–0.3 \times 10^{-2}$ in both [MnCu] and [MnNi] Heisenberg chains, in good agreement with structural findings.

In view of the close values of J found in [MnNi] and [MnCo] one could expect, according to the above expression, comparable T_c values. Nevertheless, the critical temperature of [MnCo] is 60% higher (see Table I). This disagreement may come from the large exchange anisotropy exhibited by the [MnCo] chain. Thus, it is well known that lowering the symmetry of the interaction (from Heisenberg to Ising) has the effect of reducing the short-range order contributions. In other words, 1-d short-range order effects extent over a shorter temperature region as the anisotropy rises; consequently, the 3-d ordering will occur at a higher temperature in the Ising system than in the corresponding Heisenberg one with identical J and j values. The above comparison provides a clear example of the influence of the exchange anisotropy on the occurrence of the long-range magnetic ordering.

Acknowledgment. This work was supported in part by the European Economic Community (Grant ST2/164) and the Comision Interministerial de Investigacion en Ciencia y Tecnologia. EPR measurements were performed in the Chemistry Department of Florence within the framework of an Italo–Spanish collaboration (Grant 13/17).

Registry No. $MnCo(EDTA)\cdot 6H_2O$, 63502-14-7; $MnNi(EDTA)\cdot 6H_2O$, 63502-16-9; $MnCu(EDTA)\cdot 6H_2O$, 63657-85-2.

(29) See: Kahn, O., in ref 26.

(30) Richards, P. M. *Phys. Rev. B* **1984**, *10*, 4687.